

Thermal stability and crystallization kinetics of Se–Te–Sn alloys using differential scanning calorimetry

DSC study of $\text{Se}_{92}\text{Te}_{8-x}\text{Sn}_x$ ($x = 0, 1, 2, 3, 4, 5$) chalcogenide glasses

Rajneesh Kumar · Pankaj Sharma ·
P. B. Barman · Vineet Sharma · S. C. Katyal ·
V. S. Rangra

Received: 18 August 2011 / Accepted: 8 November 2011 / Published online: 25 November 2011
© Akadémiai Kiadó, Budapest, Hungary 2011

Abstract The present article deals with the differential scanning calorimetric (DSC) study of Se–Te glasses containing Sn. DSC runs are taken at four different heating rates (10, 15, 20 and 25 K min⁻¹). The crystallization data are examined in terms of modified Kissinger, Matusita equations, Mahadevan method and Augis and Bennett approximation for the non-isothermal crystallization. The activation energy for crystallization (E_c) is evaluated from the data obtained at different heating rates. Activation energy of glass transition is calculated by Kissinger's relation and Moynihan theory. The glass forming tendency is also calculated for each composition. The glass transition temperature and peak crystallization temperature increases with the increase in Sn % as well as with the heating rate.

Keywords Chalcogenides · Glass transitions · Activation energy

Introduction

Chalcogenide glasses exhibit many useful properties and have drawn a great deal of attention because of their use in

various solid-state devices like phase change memory devices, photovoltaic devices, infrared filters, xerographic machines and X-ray imaging [1–3]. The crystallization of chalcogenide glasses plays an important role in determining their transport mechanisms, thermal stability and practical applications. Kinematical studies give important conclusions for the suitable usage of a chalcogenide glass in the proper application field [4]. Different techniques have been used to study the structure of chalcogenide glasses, e.g. scanning electron microscopy (SEM), X-ray diffraction (XRD), differential scanning calorimetry (DSC) [5–7].

Calorimetric transformations in the solid state can be investigated by isothermal or non-isothermal techniques [8–11]. In the isothermal method, the sample is brought quickly to a temperature above the glass transition temperature (T_g) and the heat evolved during the crystallization process is recorded as a function of time. In the non-isothermal method, the sample is heated at a constant rate and the heat evolved is again recorded as a function of temperature or time. In isothermal method, there is disadvantage of reaching a test temperature instantaneously and, during the time in which the system needs to stabilize, no measurements are possible. A constant heating method (non-isothermal method) does not have this drawback [12]. Thus, we have used non-isothermal DSC technique for the study of glass transition kinetics in our present study.

Se–Te alloys have higher photosensitivity, higher crystallization temperature and greater hardness [13, 14]. The properties of binary alloys (Se–Te) can be varied by adding a third element from Group IV or V of the periodic table for required purpose. In our present study, thermal study and glass transition kinematics have been reported for $\text{Se}_{92}\text{Te}_{8-x}\text{Sn}_x$ ($x = 0, 1, 2, 3, 4, 5$) glassy system. Sn is added at the cost of Te and act as a chemical modifier. The

R. Kumar · V. S. Rangra
Department of Physics, Himachal Pradesh University,
Summer-Hill, Shimla 171005, Himachal Pradesh, India

P. Sharma (✉) · P. B. Barman · V. Sharma
Department of Physics, Jaypee University of Information
Technology, Waknaghat, Solan 173215,
Himachal Pradesh, India
e-mail: pks_phy@yahoo.co.in; pankaj.sharma@juit.ac.in

S. C. Katyal
Department of Physics, Jaypee Institute of Information
Technology, Noida, Uttar Pradesh, India

glass formation region of Sn-based binary and ternary chalcogenide glasses is very narrow and corresponds to small amount of Sn in the alloy [15]. From the heating rate dependence of T_g and T_p , the activation energies for glass transition and crystallization have been evaluated.

Experimental details

Bulk samples of $\text{Se}_{92}\text{Te}_{8-x}\text{Sn}_x$ ($x = 0, 1, 2, 3, 4, 5$) were prepared by the conventional melt quenching technique. The appropriate amounts of constituent elements of 99.999% purity were weighed and sealed in a quartz ampoule under a vacuum of 10^{-5} mbar. Then the sealed ampoule was placed and heated in a vertical furnace to about 900 °C, at a heating rate of 3–4 °C min^{-1} . The ampoule was inverted at regular intervals of time for nearly 8 h in order to ensure homogeneous mixing of the constituents. Then the melt was quenched in ice water to obtain glassy samples. The material was separated from the ampoule by dissolving it in a solution of HF + H_2O_2 for 48 h. Using this as source material, X-ray diffraction (XRD) studies were performed to confirm the amorphous nature of the as-prepared samples. A DSC instrument, Mettler Toledo Stare System, was used to measure T_g and T_c of the samples with a heating rate of 10, 15, 20 and 25 °C min^{-1} . About 10 mg of the powdered sample was taken in an Al pan with an empty Al pan as reference. All the samples were scanned in the temperature range between 25 and 500 °C under flowing N_2 atmosphere. The glass transition temperature was taken as the temperature corresponding to the intersection of the two linear portions adjoining the transition elbow, whereas the onset of the crystallization exotherm was used for the determination of T_c and peak of crystalline is taken as T_p . Using these values, activation energy of glass transition (E_g) and activation energy for crystallization (E_c) have been calculated.

Results and discussion

XRD pattern of $\text{Se}_{92}\text{Te}_4\text{Sn}_4$ (as reference) is shown in Fig. 1. Figure 1 confirms the amorphous nature of the samples under investigation.

Evaluation of glass transition temperature (T_g), crystallization temperature (T_c) and peak crystallization temperature (T_p)

Figure 2 shows the DSC thermograms for $\text{Se}_{92}\text{Te}_{8-x}\text{Sn}_x$ ($x = 0, 1, 2, 3, 4, 5$) at a particular heating rate of 10 °C min^{-1} . It is clear from these figures that well-defined endothermic peaks are observed at glass transition

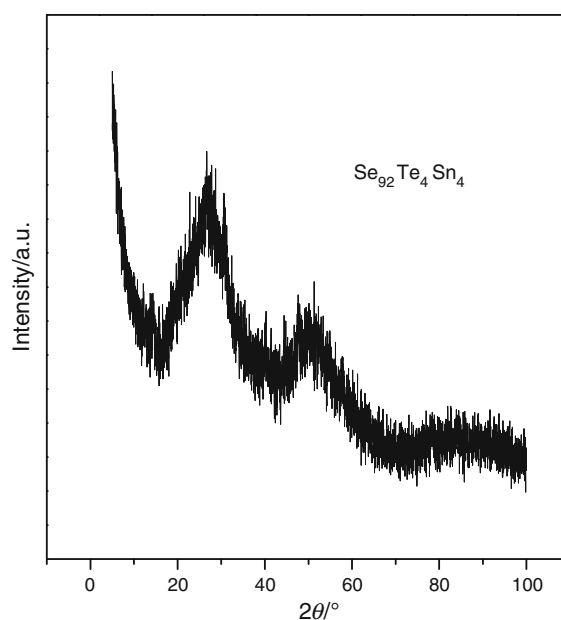


Fig. 1 X-ray diffraction pattern of $\text{Se}_{92}\text{Te}_4\text{Sn}_4$ glassy alloy

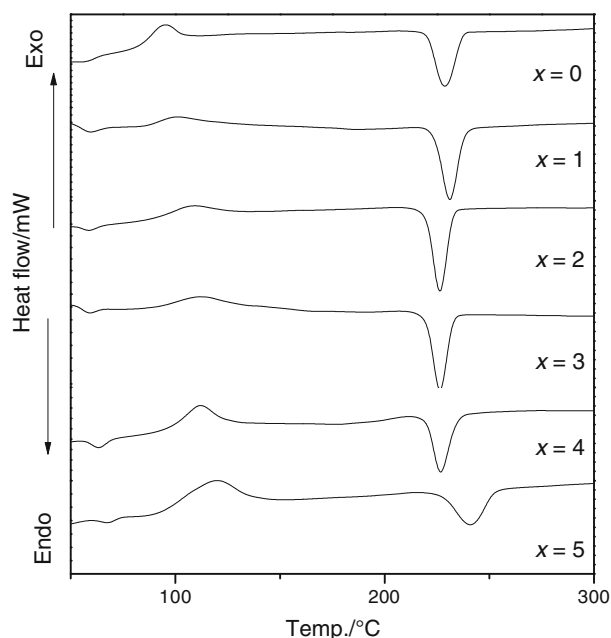


Fig. 2 DSC thermograms of $\text{Se}_{92}\text{Te}_{8-x}\text{Sn}_x$ ($x = 0, 1, 2, 3, 4, 5$) glassy alloys at single heating rate (10 °C min^{-1})

temperature (T_g), crystallization temperature (T_c), peak of crystallization (T_p) and melting temperature (T_m). Similar DSC thermograms were observed at other heating rates (not shown here). In all the DSC traces T_g was taken as the temperature corresponding to the intersection of the two linear portion adjoining the transition elbow. T_c is the temperature corresponding to the onset of crystallization and T_p as the peak crystalline temperature. The values of

Table 1 Different values of T_g , T_c , T_p , K_{gl} and T_{rg} for $\text{Se}_{92}\text{Te}_{8-x}\text{Sn}_x$ ($x = 0, 1, 2, 3, 4, 5$) glassy alloys at different heating rate (10, 15, 20 and 25 °C min^{-1})

x	$\beta/\text{K min}^{-1}$	T_g/K	T_c/K	T_p/K	T_m/K	K_{gl}	T_{rg}
0	10	320.75	353.27	367.82	490.35	0.237	0.654
	15	323.69	356.78	371.78	490.65	0.247	0.659
	20	324.95	357.05	374.55	490.45	0.24	0.662
	25	328.35	360.85	377.65	490.95	0.249	0.668
1	10	322.69	356.85	375.35	490.35	0.255	0.658
	15	324.55	365.75	382.61	487.65	0.337	0.665
	20	325.35	371.83	386.05	488.85	0.395	0.665
	25	328.95	372.35	388.95	489.75	0.369	0.671
2	10	324.35	357.75	380.35	488.15	0.256	0.664
	15	325.65	367.25	386.05	488.65	0.342	0.666
	20	327.7	367.95	389.65	488.95	0.332	0.67
	25	330.01	369.85	393.75	488.65	0.335	0.675
3	10	325.69	364.35	385.37	488.75	0.31	0.666
	15	328.95	368.85	392.14	490.65	0.327	0.67
	20	330.45	374.85	394.9	490.45	0.384	0.673
	25	330.75	374.35	397.85	491.05	0.373	0.673
4	10	328.7	365.75	386.65	491.85	0.293	0.668
	15	330.45	371.85	393.65	490.95	0.347	0.673
	20	332.55	376.55	395.95	491.95	0.381	0.675
	25	333.22	380.65	399.55	492.45	0.373	0.678
5	10	334.75	366.45	392.45	496.15	0.244	0.674
	15	336.65	372.55	397.35	496.65	0.289	0.677
	20	337.75	371.05	400.15	497.25	0.263	0.679
	25	339.48	374.85	402.45	499.15	0.284	0.68

T_g , T_c and T_p of all the composition are given in the Table 1.

Compositional and heating rate dependence of glass transition temperature

The heating rate (β) dependence of the glass transition temperature is shown in Fig. 3. From Fig. 3, it is clear that the value of T_g increases with increase in heating rate. The heating rate dependence of T_g can be expressed in terms of the following empirical relation

$$T_g = A + B \ln \beta \quad (1)$$

where A and B are constants. The value of A indicates the glass transition temperature for the heating rate of 1 K min^{-1} . It has been found by various workers [16] that the slope B in Eq. 1 is related to the cooling rate of the melt, i.e. both are proportional to each other. The physical significance of B related with the response of the configurational changes within the glass transformation region. The values of A and B for different alloys are given in

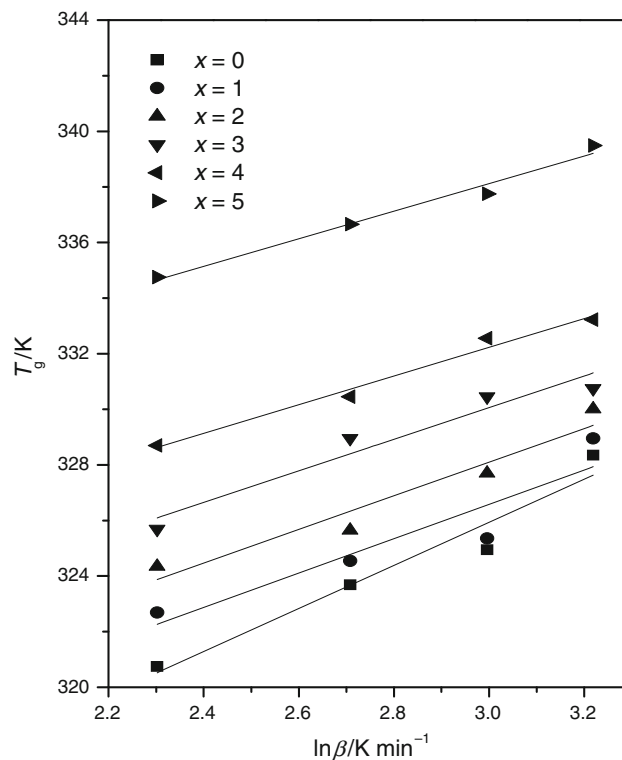
**Fig. 3** Plots of T_g vs. $\ln(\beta)$ of $\text{Se}_{92}\text{Te}_{8-x}\text{Sn}_x$ ($x = 0, 1, 2, 3, 4, 5$) alloys

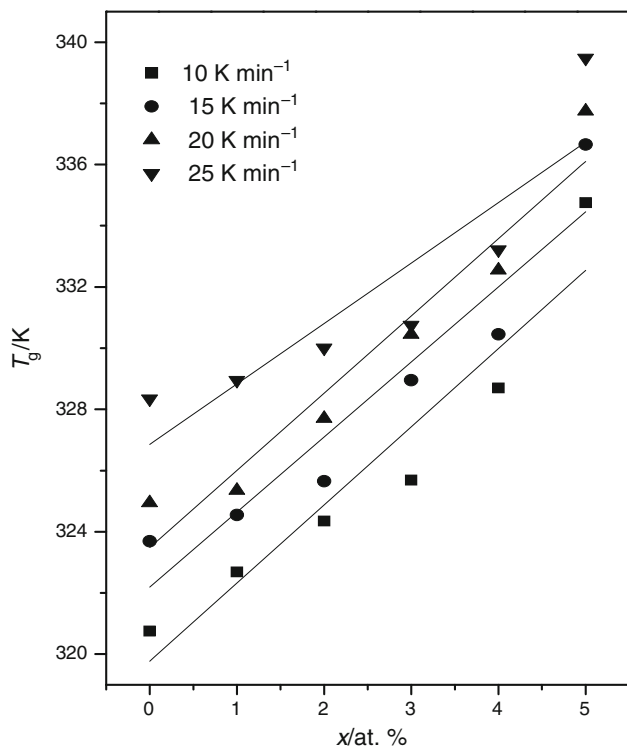
Table 2. The values of B for glassy $\text{Se}_{92}\text{Te}_{8-x}\text{Sn}_x$ ($x = 0, 1, 2, 3, 4, 5$) is found to vary from 4 to 8. This change implies that structural changes takes place in the glassy samples with the change in composition [17].

The compositional dependence of glass transition temperature (T_g) is shown in Fig. 4. It is clear that with the increase in Sn concentration, T_g increases. This indicates that the addition of Sn to the Se–Te system cross-links the already existing Se–Te chains thus forming a cross-linked structure which leads the structure towards more rigidity resulting in an increase in the T_g of the material [18]. The increase in T_g with heating rate is explained by the fact that when the heating rate increases, the system does not have sufficient time for nucleation and crystallization to occur.

The observed behaviour in T_g and T_c can be visualized by using the chemical ordered network (CON) model by Ovshinsky et al. [19]. The values of homopolar bond energies for Se, Te and Sn are (44, 33 and 34.2 kcal mol^{-1}) respectively [20]. The heteropolar bond energies for Sn–Se, Sn–Te and Se–Te are (49.14, 34.16 and 44.14 kcal mol^{-1}) respectively [21]. The bond energy and bond formation probability of Sn–Se bond is largest. So the observed continuous increase in the value of T_g and T_c may be due to the replacement of some weaker bonds with some stronger bonds. Thus, with the addition of Sn, the weaker Se–Se bonds are replaced by the stronger Sn–Se bonds, which results in an increase in T_g and T_c .

Table 2 Kinetic parameters (*A* and *B*) of $\text{Se}_{92}\text{Te}_{8-x}\text{Sn}_x$ ($x = 0, 1, 2, 3, 4, 5$) glassy alloys

<i>x</i>	<i>A</i>	<i>B</i>
0	302.66 ± 3.53	7.75 ± 1.25
1	308.02 ± 4.80	6.18 ± 1.69
2	309.94 ± 3.15	6.05 ± 1.11
3	313.00 ± 2.83	5.68 ± 1.00
4	316.75 ± 1.35	5.15 ± 0.47
5	323.21 ± 1.32	4.96 ± 0.46

**Fig. 4** Compositional dependence of T_g of $\text{Se}_{92}\text{Te}_{8-x}\text{Sn}_x$ ($x = 0, 1, 2, 3, 4, 5$) at different heating rates (10, 15, 20 and 25 K min^{-1})

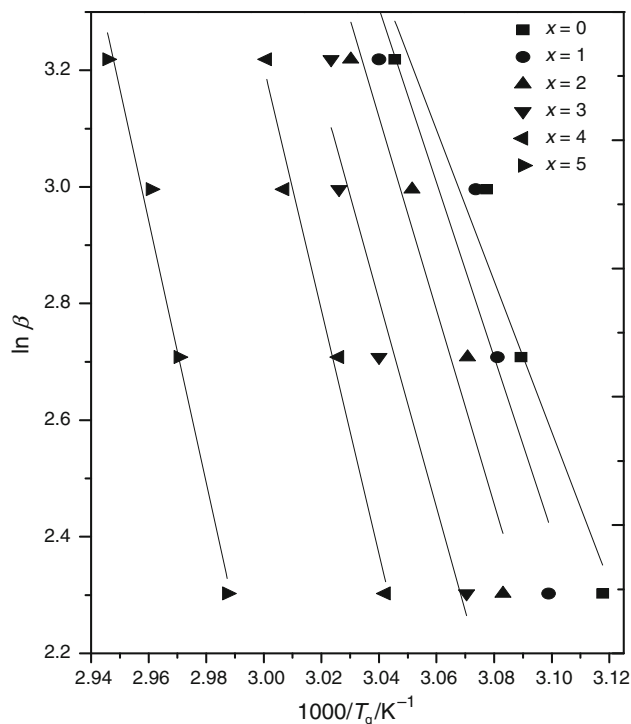
Evaluation of activation energy of glass transition (E_g)

Moynihan method

The activation energy of glass transition has been calculated using Moynihan equation. The dependence of T_g on heating rate is given by [22]

$$\frac{d(\ln \beta)}{d\left(\frac{1}{T_g}\right)} = -\frac{E_g}{R} \quad (2)$$

where R is gas constant. Equation 2 states that plot between $\ln \beta$ and T_g should be a straight line and the activation energy involved in the molecular motions and rearrangement around T_g can be calculated from the slope of this

**Fig. 5** Plots of $\ln(\beta)$ vs. $1000/T_g$ for $\text{Se}_{92}\text{Te}_{8-x}\text{Sn}_x$ ($x = 0, 1, 2, 3, 4, 5$) alloys**Table 3** Values of E_g (activation energy of glass transition) for $\text{Se}_{92}\text{Te}_{8-x}\text{Sn}_x$ ($x = 0, 1, 2, 3, 4, 5$) alloys

<i>x</i>	Activation energy of glass transition/ kJ mol^{-1}	
	Moynihan method	Kissinger method
0	107.23 ± 16	101.84 ± 16
1	124.08 ± 33	118.69 ± 33
2	137.53 ± 25	132.13 ± 25
3	147.82 ± 26	142.42 ± 26
4	173.22 ± 16	167.74 ± 16
5	186.50 ± 17	180.94 ± 17

plot. The plots of $\ln \beta$ and $1000/T_g$ are shown in the Fig. 5 for $\text{Se}_{92}\text{Te}_{8-x}\text{Sn}_x$ ($x = 0, 1, 2, 3, 4, 5$) glassy alloys. The activation energy of glass transition is calculated from the slopes of these plots. The values are shown in Table 3. It is clear that the value of E_g increases with increase in Sn concentration.

Kissinger's method

In glass transition kinematics, this method is frequently used for calculating activation energy of glass transition (E_g). Using this method the heating rate dependence of T_g is given by [23]

$$\ln\left(\frac{T_g^2}{\beta}\right) + \text{const.} = \frac{E_g}{RT_g} \quad (3)$$

E_g is calculated from the slopes of the plots between $\ln(T_g^2/\beta)$ and $1000/T_g$ (figure not shown here). The observed values are shown in Table 3. The activation energy calculated from both the approaches shows similar trends. With increase of Sn content, the glassy matrix becomes heavily cross-linked and steric hindrance increases. The Se–Se bonds will be replaced by Sn–Se bonds, which have higher bond energy. Hence, the cohesive energy of the system increases with increasing Sn content, resulting in an increase in the activation energy.

Activation energy of crystallization (E_c)

Modified Kissinger's method

The activation energy of crystallization E_c has been calculated from the variation of the peak crystallization temperature (T_p) with heating rate using the modified Kissinger's equation

$$\ln\left(\frac{T_p^2}{\beta}\right) + \text{const.} = \frac{E_c}{RT_p} \quad (4)$$

The slope of the graphs between $\ln(T_p^2/\beta)$ and $1000/T_p$ gives the value of the activation energy of crystallization (E_c) (Fig. 6). The different values for various compositions are shown in Table 4. At $x = 1$, E_c decreases and then increases for higher Sn concentration. This might be due to the following reason. There is tendency of Se containing glasses to form polymerized network and suppression of homopolar bonds [24]. With the addition of Sn, i.e. $x = 1$, chain as well as ring structures are affected and decrease in E_c . This leads to increases in speed of crystallization. With the further addition of Sn, glassy matrix become heavily cross-linked and Se–Se bonds are replaced by Sn–Se bond (having large bond energy). So it results in increase in cohesive as well as activation energy of glass crystallization.

Mahadevan method

The activation energy of crystallization according to Mahadevan method [25] can be calculated by the given formula;

$$\ln \beta = -\frac{E_c}{RT_p} + \text{const.} \quad (5)$$

The slopes of plots between $\ln(\beta)$ and $(1000/T_p)$ gives the resultant values of the activation energies (E_c). The observed values are given in Table 4. There is good agreement between Mahadevan's method and the values

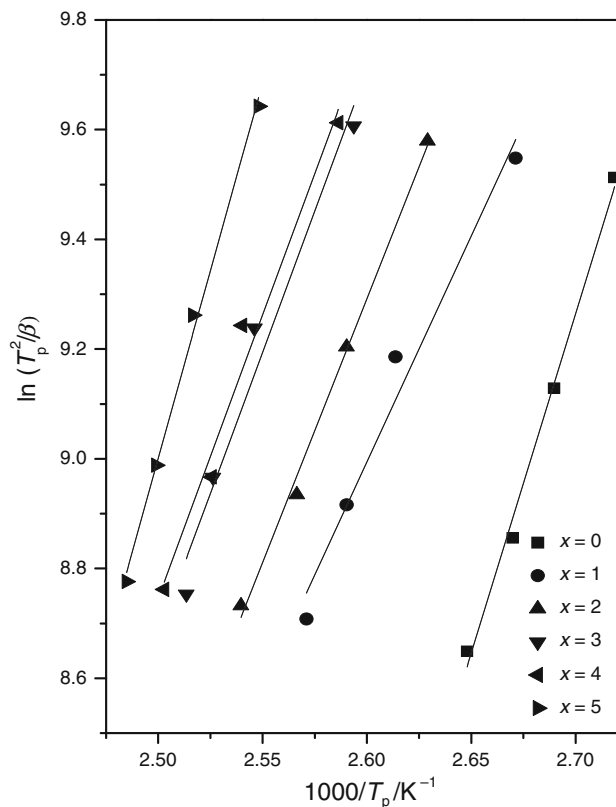


Fig. 6 Plots of $\ln(T_p^2/\beta)$ vs. $1000/T_p$ for $\text{Se}_{92}\text{Te}_{8-x}\text{Sn}_x$ ($x = 0, 1, 2, 3, 4, 5$) alloys

obtained in modified Kissinger's and Augis and Benett's method.

Matusita method

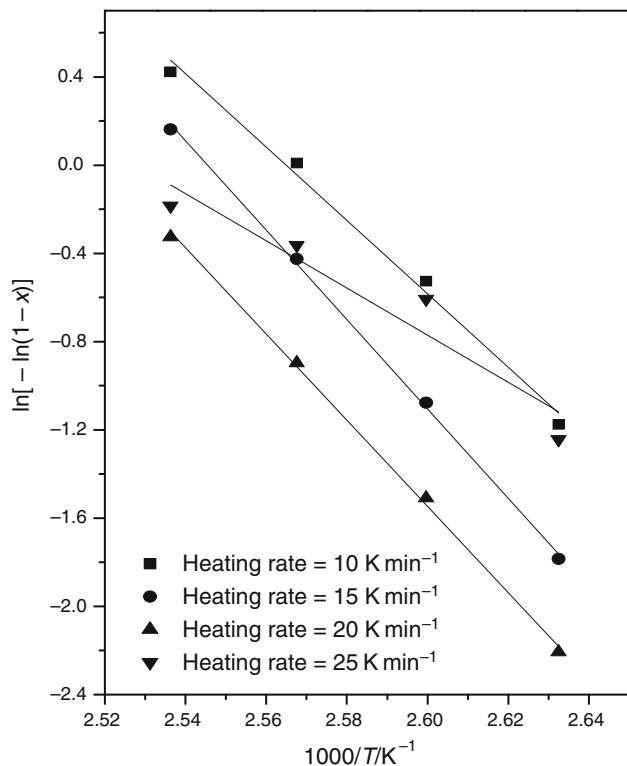
The activation energy (E_c) of the amorphous–crystalline transformation and the order of crystallization reaction (Avrami index, n) can be calculated using the Matusita relation [26]. The volume fraction of crystals (X) precipitated in a glass heated at a uniform rate (β) is related to the activation energy of crystallization (E_c) through the expression

$$\ln[-\ln(1 - X)] = -n \ln \beta - 1.052 \frac{mE_c}{RT} + \text{const.} \quad (6)$$

where X is the volume fraction of crystalline material precipitated in the glass, E_c is the activation energy of crystallization and R is the gas constant. X at a particular temperature (T) is given by A_T/A , where A is the total area under the exothermic peak and A_T is the area under the exotherm between the onset temperature of crystallization and the particular temperature (T) and m and n are integers which depend on the mechanism of the growth and the dimensionality of the crystal. When the nuclei formed during heating at a constant rate are dominant, n is equal to

Table 4 Values of E_c (activation energy of crystallization), n , m , K_0 (frequency factor) for $\text{Se}_{92}\text{Te}_{8-x}\text{Sn}_x$ ($x = 0, 1, 2, 3, 4, 5$) alloys

x	Activation energy of glass crystallization/ kJ mol^{-1}				m	n	K_0/s^{-1}
	Mod. Kissinger method	Mahadevan method	Matusita method	Augis and Bennet method			
0	102.67 ± 9	108.81 ± 9	136.15 ± 11	105.74 ± 9	1	1.58	3.08×10^{13}
1	68.39 ± 8	74.70 ± 8	106.03 ± 13	71.54 ± 8	1	1.43	2.61×10^8
2	79.84 ± 4	86.23 ± 4	96.19 ± 8	83.08 ± 4	1	1.38	7.15×10^9
3	85.40 ± 11	91.96 ± 11	99.88 ± 6	88.72 ± 11	1	1.31	2.73×10^{10}
4	85.65 ± 9	92.13 ± 9	112.38 ± 12	88.89 ± 9	1	1.75	2.76×10^{10}
5	113.54 ± 5	120.10 ± 5	139.46 ± 9	116.78 ± 5	1	1.26	9.45×10^{13}

**Fig. 7** Plots of $\ln[-\ln(1-x)]$ vs. $1000/T$ for $\text{Se}_{92}\text{Te}_4\text{Sn}_4$ glassy alloy at 10, 15, 20 and 25 K min^{-1}

($m + 1$) and when nuclei formed during any previous heat treatment prior to thermal analysis are dominant, n is equal to m .

Plots of $\ln[-\ln(1-x)]$ vs. $1000/T$ for the investigated glassy samples, were found to be linear irrespective of some points. The plot of $\ln[-\ln(1-x)]$ vs. $1000/T$ for $\text{Se}_{92}\text{Te}_4\text{Sn}_4$ at all heating rate is shown in Fig. 7. At high temperatures slight non-linear behaviour was observed (at heating rate 25 K min^{-1}). Similar kind of behaviour has been already reported for other glassy compositions [27]. This nonlinear behaviour may be due to the reason that either the crystal growth might be stopped or the nuclei get saturated. The value of mE_c was calculated from the slope of the $\ln[-\ln(1-x)]$ vs. $1000/T$ for all compositions.

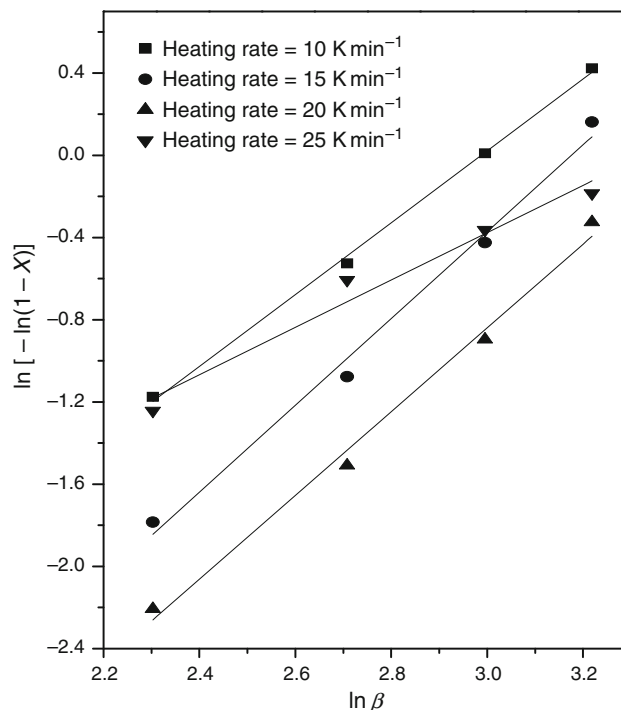
**Fig. 8** Plots of $\ln[-\ln(1-x)]$ vs. $\ln(\beta)$ for $\text{Se}_{92}\text{Te}_4\text{Sn}_4$ glassy alloy at 10, 15, 20 and 25 K min^{-1}

Figure 8 shows linear plots of $\ln[-\ln(1-x)]$ vs. $\ln(\beta)$. From the slope of these plots average value of n is calculated. All the values are reported in Table 4. A non-integer value of n means that two crystallization mechanisms are working simultaneously during the amorphous-crystalline transformation of the $\text{Se}_{92}\text{Te}_{8-x}\text{Sn}_x$ glass while integer value of n indicates that only one crystallization mechanism is responsible for the crystallization process. In our present composition, n is non-integer means two crystallization mechanisms are working simultaneously. It has been already shown that n can take the value 4, 3, 2, 1 depending upon the type of nucleation and growth. In all composition $m = 1$ which means bulk nucleation with one-dimensional growth is dominant crystallization mechanism.

The slope of the graphs plotted between $\ln[-\ln(1 - X)]$ and $1000/T$ gives mE_c . The value of E_c calculated by this method is shown in the Table 4. The values obtained by this method are quite larger in comparison to earlier discussed methods. This difference in the activation energies calculated using different models may be due to the different approximations used in the models. In addition, the temperature and pressure gradients in the sample vary randomly due to heating rate and such random variation occur in quick interval during crystallization. So they results in variation in kinetic parameters. Similar variations in the activation energy have also been reported in other chalcogenide glasses [28].

Augis and Bennett method

The activation energy for crystallization can also be deduced using the formula suggested by Augis and Bennett [29].

$$\ln \left[\frac{\beta}{T_p - T_0} \right] \cong \frac{-E_c}{RT_p} + \ln K_0 \quad (7)$$

where T_p and T_0 are peak crystallization and initial temperature, respectively. K_0 is frequency factor, which measures the probability of molecular collision effective for formation of the activated complex, was calculated from the intercept of the straight line with vertical axis. By assuming that $T_0 \gg T_p$; Eq. 7 can be approximated to the following form:

$$\ln \left[\frac{\beta}{T_p} \right] \cong \frac{-E_c}{RT_p} + \ln K_0 \quad (8)$$

The relation between $\ln \beta$ vs. $1000/T_p$ gives a straight line (figure not shown here). The calculated values of E_c for different compositions are shown in Table 4. The values obtained by this method are in good agreement to Eqs. 4 and 5. The corresponding values of the frequency factors (K_0) are also shown in Table 4.

Glass forming tendency

The difference between T_c and T_g , which is an indication of thermal stability of the glasses, increases linearly with the increase in Sn content except $x = 5$ at.%. The difference ($T_c - T_g$) also increases with increase in heating rate, means thermal stability increases. For $x = 4$ at.%, it is maximum, means large thermal stability. The thermal stability and ease of glass formation have great importance in memory and switching materials. The glass forming tendency can be calculated from the formula given by Hurby [30].

$$K_{gl} = \frac{T_c - T_g}{T_m - T_c} \quad (9)$$

All the values of K_{gl} are reported in Table 1. For $x = 0$ and 5, K_{gl} is minimum, means they are best materials for phase change optical recording.

The ease of glass formation is determined by calculating T_{rg} (reduced glass transition temperature) [31].

$$T_{rg} = \frac{T_g}{T_m} \quad (10)$$

The observed values of T_{rg} in all compositions obey 2/3 rule; which means $T_g/T_m = 2/3$. The values of K_{gl} and T_{rg} for $\text{Se}_{92}\text{Te}_{8-x}\text{Sn}_x$ ($0 \leq x \leq 5$) are given in Table 1.

Conclusions

Calorimetric measurements have been performed in $\text{Se}_{92}\text{Te}_{8-x}\text{Sn}_x$ ($x = 0, 1, 2, 3, 4, 5$) glassy alloys. DSC scans of these alloys show the well-defined endothermic peak at glass transition temperature T_g and peak crystallization temperature T_p . It has been found that the glass transition temperature increases with increase in the concentration of Sn. This increase in T_g is explained in terms of chemically ordered network model (CONM). The activation energy of glass transition E_g has been calculated by Kissinger's and Moynihan's relation for various glassy alloys. There is good agreement between these two approaches. The activation energy of glass crystallization (E_c) is calculated by four different approaches (modified Kissinger, Mahadevan, Motusita and Augis and Bennett method). The thermal stability and glass forming ability of each composition has also been calculated. The thermal stability and ease of glass formation might be the importance of these alloys in memory and switching applications.

References

1. Kumar H, Mehta N, Kumar A. Effect of some chemical modifiers on the glass/crystal transformation in binary $\text{Se}_{90}\text{In}_{10}$ alloy. *J Therm Anal Calorim.* 2011;103:903–9.
2. Aly AK, Dahshan A, Abdel-Rahim FM. Thermal stability of Ge–As–Te–In glasses. *J Alloys Compd.* 2009;470:574–9.
3. Lian ZG, Pan W, Furniss D, Benson TM, Seddon AB, Kohoutek T, Orava J, Wagner T. Embossing of chalcogenide glasses: monomode rib optical waveguides in evaporated thin films. *Opt Lett.* 2009;34:1234–6.
4. Kumar R, Sharma P, Rangra VS. Kinetic studies of bulk $\text{Se}_{92}\text{Te}_{8-x}\text{Sn}_x$ ($x = 0, 1, 2, 3, 4$ and 5) semiconducting glasses by DSC technique. *J Therm Anal Calorim.* 2011. doi:10.1007/s10973-011-1661-z.
5. Savage JA. *Infrared optical materials and their antireflection coatings.* Bristol: Adam Hilger; 1985.
6. Choi D, Madden S, Bulla D, Wang R, Rode A, Luther-Davies B. Thermal annealing of arsenic tri-sulphide thin film and its influence on device performance. *J Appl Phys.* 2010;107:053106. doi: 10.1063/1.3310803 (6 pages).

7. Tanaka K. Structural phase transitions in chalcogenide glasses. *Phys Rev B*. 1989;39:1270–9.
8. Sharma A, Barman PB. Effect of Bi incorporation on the glass transition kinetics of $\text{Se}_{85}\text{Te}_{15}$ glassy alloy. *J Therm Anal Calorim*. 2009;96:413–7.
9. Rysava N, Spasov T, Tichy L. Isothermal DSC method for evaluation of the kinetics of crystallization in the Ge-Sb-S glassy system. *J Therm Anal*. 1987;32:1015–21.
10. Giridhar A, Mahadevan S. Studies on the As-Sb-Se glass system. *J Non-Cryst Solids*. 1982;51:305–15.
11. Afify N. Differential scanning calorimetric study of chalcogenide glass $\text{Se}_{0.7}\text{Te}_{0.3}$. *J Non-Cryst Solids*. 1991;128:279–84.
12. Strink MJ, Zahra AM. Determination of the transformation exponent s from experiments at constant heating rate. *Thermochim Acta*. 1997;298:179–89.
13. Majeed Khan MA, Zulfequar M, Husain M. Optical investigation of $a\text{-Se}_{100-x}\text{Bi}_x$ alloys. *J Opt Mater*. 2003;22:21–9.
14. Sharma P, Katyal SC. Effect of tellurium addition on the optical behaviour of germanium selenide glassy semiconductors. *Phys B*. 2008;403:3667–71.
15. Kumar H, Mehta N, Singh K. Calorimetric studies of glass transition phenomenon in glassy $\text{Se}_{80-x}\text{Te}_{20}\text{Sn}_x$. *Phys Scr*. 2009;80. doi:10.1088/0031-8949/80/06/065602.
16. Lezal D, Zavadil J, Prochazka M. Sulfide, selenide and telluride glassy systems for optoelectronic applications. *J Optoelectron Adv Mater*. 2005;7:2281–91.
17. Lasocka M. The effect of scanning rate on glass transition temperature of splat-cooled $\text{Te}_{85}\text{Ge}_{15}$. *Mater Sci Eng*. 1976;23:173–7.
18. Kaur G, Thangaraj R, Komatsu T. Crystallization kinetics of bulk amorphous Se–Te–Sn system. *J Mater Sci*. 2001;36:4530–3.
19. Bicerno J, Ovshinsky SR. Chemical bond approach to the structures of chalcogenide glasses with reversible switching properties. *J Non-Cryst Solids*. 1985;74:75–84.
20. Williams RJP, Fraústo da Silva JJR. The natural selection of chemical elements: the environment and life's chemistry. New York: Oxford University Press Inc.; 1997. p. 58.
21. Kumar R, Sharma P, Katyal SC, Sharma P, Rangra VS. A study of Sn addition on bonding arrangement of Se–Te alloys using far infrared transmission spectroscopy. *J Appl Phys*. 2011;110. doi:10.1063/1.3603010 (5 pages).
22. Mohynihan CT, Eastal AJ, Wilder J, Tucker J. Dependence of the glass transition temperature on heating and cooling rate. *J Phys Chem*. 1974;78:2673–7.
23. Kissinger HE. Variation of peak temperature with heating rate in differential thermal analysis. *J Res Mater Bur Stand*. 1956;57:217–21.
24. Mehra RM, Kaur G, Mathur PC. Crystallization kinetics of bulk amorphous $\text{Se}_{80-x}\text{Sb}_x\text{Te}_{20}$. *J Mater Sci*. 1991;26:3433–7.
25. Mahadevan S, Giridhar A, Singh AK. Calorimetric measurements on As-Sb-Se glasses. *J Non-Cryst Solids*. 1986;88:11–34.
26. Matusita K, Konatsu T, Yokota R. Kinetics of non-isothermal crystallization process and activation energy for crystal growth in amorphous materials. *J Mater Sci*. 1984;19:291–6.
27. Deepika, Rathore KS, Saxena NS. A kinetic analysis of non-isothermal glass-crystal transformation in $\text{Ge}_{1-x}\text{Sn}_x\text{Se}_{2.5}$ ($0 \leq x \leq 0.5$) glasses. *J Phys Condens Matter*. 2009;21. doi:10.1088/0953-8984/21/33/335102.
28. Chander R, Thangaraj R. Thermal and optical analysis of Te substituted Sn–Sb–Se chalcogenide semiconductors. *Appl Phys A*. 2010;99:181–7.
29. Augis JA, Bennett JE. Calculation of the Avrami parameters for heterogeneous solid state reactions using a modification of the Kissinger method. *J Therm Anal*. 1978;13:283–92.
30. Hruby A. Evaluation of glass-forming tendency by means of DTA. *Czech J Phys B*. 1972;22:1187–93.
31. Kauzmann W. The nature of the glassy state and the behavior of liquids at low temperatures. *Chem Rev*. 1948;43:219–56.